ORIGINAL RESEARCH

Tat peptide-decorated gelatin-siloxane nanoparticles for delivery of CGRP transgene in treatment of cerebral vasospasm

Xin-Hua Tian[1,2]
Zhi-Gang Wang[1,2]
Han Meng[1,2]
Yu-Hua Wang[2]
Wei Feng[2]
Feng Wei[2]
Zhi-Chun Huang[2]
Xiao-Ning Lin[2]
Lei Ren[3,4]

[1]Xiehe Clinical College of Medicine, Fujian Medical University, Fuzhou, [2]Department of Neurosurgery, Zhongshan Hospital, [3]Research Center of Biomedical Engineering, Department of Biomaterials, College of Materials, [4]State Key Laboratory for Physical Chemistry of Solid Surfaces, Xiamen University, Xiamen, People's Republic of China

Background: Gene transfer using a nanoparticle vector is a promising new approach for the safe delivery of therapeutic genes in human disease. The Tat peptide-decorated gelatin-siloxane (Tat-GS) nanoparticle has been demonstrated to be biocompatible as a vector, and to have enhanced gene transfection efficiency compared with the commercial reagent. This study investigated whether intracisternal administration of Tat-GS nanoparticles carrying the calcitonin gene-related peptide (CGRP) gene can attenuate cerebral vasospasm and improve neurological outcomes in a rat model of subarachnoid hemorrhage.

Method: A series of gelatin-siloxane nanoparticles with controlled size and surface charge was synthesized by a two-step sol-gel process, and then modified with the Tat peptide. The efficiency of Tat-GS nanoparticle-mediated gene transfer of pLXSN-CGRP was investigated in vitro using brain capillary endothelial cells and in vivo using a double-hemorrhage rat model. For in vivo analysis, we delivered Tat-GS nanoparticles encapsulating pLXSN-CGRP intracisternally using a double-hemorrhage rat model.

Results: In vitro, Tat-GS nanoparticles encapsulating pLXSN-CGRP showed 1.71 times higher sustained CGRP expression in endothelial cells than gelatin-siloxane nanoparticles encapsulating pLXSN-CGRP, and 6.92 times higher CGRP expression than naked pLXSN-CGRP. However, there were no significant differences in pLXSN-CGRP entrapment efficiency and cellular uptake between the Tat-GS nanoparticles and gelatin-siloxane nanoparticles. On day 7 of the in vivo experiment, the data indicated better neurological outcomes and reduced vasospasm in the subarachnoid hemorrhage group that received Tat-GS nanoparticles encapsulating pLXSN-CGRP than in the group receiving Tat-GS nanoparticles encapsulating pLXSN alone because of enhanced vasodilatory CGRP expression in cerebrospinal fluid.

Conclusion: Overexpression of CGRP attenuated vasospasm and improved neurological outcomes in an experimental rat model of subarachnoid hemorrhage. Tat-GS nanoparticle-mediated CGRP gene delivery could be an innovative strategy for treatment of cerebral vasospasm after subarachnoid hemorrhage.

Keywords: gene transfer, nanoparticles, calcitonin gene-related peptide, cerebral vasospasm

Introduction

Cerebral vasospasm is the delayed narrowing of large capacitance arteries at the base of the brain after subarachnoid hemorrhage, and is the leading cause of mortality and disability in patients who have suffered this type of hemorrhage. Vasospasm typically occurs 3–5 days after subarachnoid hemorrhage, with maximal narrowing at 7–10 days and a gradual resolution over 2–3 weeks.[1] Current therapeutic options include oral administration of nimodipine (a calcium antagonist), hypervolemia-hemodilution-hypertension therapy, and intracranial angioplasty. However, because

Correspondence: Xin-Hua Tian
Department of Neurosurgery, Zhongshan Hospital, Xiamen University, 209 South Hubin Road, Xiamen 361004, People's Republic of China
Tel +86 59 2229 2352
Fax +86 59 2221 2328
Email txhmd@yahoo.com.cn

865

of the multiple and complex mechanisms of vasospasm, no effective clinical method for prevention has yet been demonstrated. Gene therapy targeted at the level of cellular gene expression represents a new approach to the treatment of cerebrovascular disease, which may hold great potential for the treatment of cerebral vasospasm.

Calcitonin gene-related peptide (CGRP) is a potent arterial and venous vasodilator, which has shown encouraging results in the prevention of vasospasm after subarachnoid hemorrhage in clinical therapy. CGRP interacts with the $CGRP_1$ receptor on endothelial and smooth muscle cells and stimulates adenylate cyclase to produce cAMP via endothelium-dependent or endothelium-independent signaling pathways, leading to vascular relaxation.[2] It has been reported that injecting recombinant adenovirus encoding the prepro-CGRP gene into the cisterna magna is effective in the prevention of vasospasm after subarachnoid hemorrhage in rabbits and dogs.[3,4] In both animal studies, histologically and angiographically determined end points were used, but neither study reported the neurological outcomes for the animals, which is a limitation found in many studies involving animal models of subarachnoid hemorrhage.[5] Further, the inflammatory and immune responses, which are the most serious problems caused by administration of recombinant adenovirus into intracerebrospinal fluid,[6,7] would prevent use of this approach in patients.

Nanoparticles as vectors have been the focus of extensive research in gene delivery and expression because of their low toxicity, biodegradability, and biocompatibility.[8–10] Because nanoparticles cannot integrate into the host genome, they do not have toxicity or provoke an immune response, and would be expected to have a short-term action. The period of risk of vasospasm is 2–3 weeks at the most, so nanoparticles would be advantageous and useful in the treatment of this condition which requires only transient gene expression. In a previous study, gelatin-siloxane (GS) nanoparticles with a controlled size and surface charge were synthesized using a two-step sol-gel process and decorated with HIV-derived Tat peptide-decorated gelatin-siloxane (Tat-GS) nanoparticles via sulfhydryl groups, and we hypothesized that these nanoparticles would be biocompatible as vectors and could enhance gene transfection efficiency compared with that of the commercial reagent, Lipofectamine™.[11,12] However, it had not been investigated whether Tat-GS nanoparticle-mediated CGRP gene delivery could achieve satisfactory prevention of vasospasm and improve the neurological outcome.

In this study, we investigated whether Tat-GS nanoparticles loaded with the CGRP gene can reduce vasospasm and improve the neurological outcome in a rat model of subarachnoid hemorrhage. Tat-GS nanoparticle-mediated CGRP gene delivery is an innovative strategy for the treatment of vasospasm after subarachnoid hemorrhage.

Materials and methods
Cell culture
An hCMEC/D3 endothelial cell line derived from the human brain was obtained from Beina Chuanglian Biotechnology Research Institute (Beijing, People's Republic of China) and cultured in RPMI-1640 medium supplemented with 10% fetal bovine serum and 1% penicillin-streptomycin. The cells were routinely maintained as stationary cultures in Petri dishes, and incubated at 37°C in a controlled environment with 5% CO_2.

Construction of plasmid DNA
Rat CGRP cDNA was amplified by polymerase chain reaction and then inserted into the expression plasmid vector pLXSN (pLXSN-CGRP). pDNA (pLXSN and pLXSN-CGRP) was propagated in *Escherichia coli DH5α* and purified using a TIANprep Midi Plasmid kit (Tiangen Biotech Co, Ltd, Beijing, People's Republic of China). Purity and concentration were confirmed by measuring absorbance at 260 nm and 280 nm on a DU 800 spectrophotometer (Beckman Coulter Inc, Fullerton, CA, USA) and by agarose gel electrophoresis.

Preparation of nanoparticles
GS and Tat-GS nanoparticles were prepared according to previously reported methods.[11,13] Briefly, 0.2 g of 3-glycidoxypropyl-trimethoxysilane (Acros Organics, Fair Lawn, NJ, USA) was added to 1% gelatin solution in HCl (pH 3.0) at 60°C with stirring for 30 minutes. Next, 0.08 g of 3-aminopropyl-trimethoxysilane (Acros Organics) was added into the above solution. Continuous stirring for 7–10 hours at 60°C produced a milky emulsion. The resulting GS nanoparticles were then obtained by centrifugation (13,000 rpm, 20°C, 20 minutes) and ultrasonic washing three times with deionized water. A sulfhydryl group was then introduced onto the surfaces of the GS nanoparticles using N-succinimidyl-3-(2-pyridyldithio) propionate (Pierce Biotechnology Inc, Rockford, IL, USA). Tat peptide (KYGRRRQRRKKRGC, Chinese Peptide Company, Hangzhou, People's Republic of China) with a free sulfhydryl group at the end of the strand was subsequently coupled to the nanoparticles via a disulfide bond at a Tat to GS nanoparticle ratio of 1.58 µmol/g.

Tat-GS nanoparticles were finally obtained by centrifugation (20 minutes, 20°C, 13,000 rpm) and washing three times with deionized water.

Preparation of nanoparticle-pDNA complexes

Nanoparticles encapsulating pDNA (GS NP-pDNA and Tat-GS NP-pDNA) were prepared by electrostatic interaction. Nanoparticle suspensions were mixed with pDNA solution at a nanoparticle to pDNA weight ratio of 100:1, followed by 30 seconds of vortexing and one hour of incubation. Centrifugation (13,000 rpm, 20°C, 20 minutes) and ultrasonic washing three times with deionized water yielded the purified nanocomplexes. The GS NP-pDNA complexes and Tat-GS NP-pDNA complexes were redispersed in deionized water and stored at −4°C for the following experiments.

Characterization of nanoparticles

Integration of the Tat peptide into the GS nanoparticles was confirmed by spectrofluorimetric quantitative analysis. For fluorescence measurements, FITC-labeled Tat peptide was used in the synthesis processing. The supernatant of the resulting FITC-Tat-GS nanoparticle suspension was collected by centrifugation (13,000 rpm, 20°C, 20 minutes). Next, the FITC-Tat-GS nanoparticles were redispersed in deionized water and the supernatant was analyzed using a fluorescence spectrophotometer (Hitachi 650–10s, Toyokawa, Japan). The excitation and emission wavelengths were 490 nm and 520 nm, respectively. Observation of the GS and Tat-GS nanoparticles was done using a transmission electron microscope (2100 HC, JEOL, Tokyo, Japan) at an operating voltage of 200 kV in bright-field mode. Dilute suspensions of nanoparticles in water were dropped onto a copper grid and then air-dried for analysis by transmission electron microscopy. The mean diameter and zeta potential of the nanoparticles were measured using a dynamic light scattering detector (Nano-ZS Zetasizer, Malvern Instruments, Worcestershire, UK).

Gel retardation assay

The entrapment efficiency of pLXSN-CGRP incorporated into nanoparticles was evaluated by gel electrophoresis. First, 10 μL of nanocomplexes (GS nanoparticles encapsulating pLXSN-CGRP and Tat-GS nanoparticles encapsulating pLXSN-CGRP 2.5 mg/mL) were mixed with 2 μL of 6× loading buffer and loaded onto 1% agarose gel with ethidium bromide 500 ng/mL, then run with Tris-acetate buffer at 150 V for 45 minutes. pLXSN-CGRP retardation

was observed by irradiation using a molecular imaging device (Gel Doc XR, Bio-Rad, Mississauga, ON, Canada).

MTT assay

The in vitro cytotoxicity of GS and Tat-GS nanoparticles was analyzed by MTT assay. The hCMEC/D3 cells were seeded at a density of 1×10^5 cells/well in polystyrene 96-well culture plates, and incubated at 5% CO_2 and 37°C for 24 hours to enable cell attachment. After removing the culture medium, 100 μL of serum-free RPMI-1640 medium containing the GS or Tat-GS nanoparticles (at concentrations of 100 μg/mL, 300 μg/mL, and 500 μg/mL) was added to each well. Cells treated with medium only served as a negative control group. After 24 hours of coincubation, the medium was replaced with 20 μL of MTT solution (5 mg/mL in phosphate-buffered solution) and cultured for a further 4 hours. At the end of the assay, the MTT solution was removed and 100 μL of dimethylsulfoxide was added to dissolve the formazan crystals that had formed. The plate was incubated for an additional 30 minutes before determination at 570 nm in a spectrophotometric microplate reader (Bio-Tek ELX800, Winooski, VT, USA). All experiments were repeated five times, and the relative cell viability (%) was expressed as a percentage relative to the control cells.

Cellular uptake

For flow cytometry analysis, a 0.1 mg/mL solution of pLXSN-CGRP was mixed with a 0.1 mg/mL aqueous solution of propidium iodide (PI) at a volume ratio of 1:0.7, and maintained at room temperature protected from light for 20 minutes. Single-staining NP-pDNA complexes were then prepared by mixing PI-labeled pLXSN-CGRP with the nanoparticles, following preparation of the NP-pDNA complexes. The hCMEC/D3 cells were first seeded in six-well plates at 2×10^5 cells/well and incubated overnight with 5% CO_2 at 37°C. After washing three times with phosphate-buffered saline, the cells were incubated with different single-staining materials (naked PI-labeled pLXSN-CGRP, PI-labeled GS NP-pLXSN-CGRP, and PI-labeled Tat-GS NP-pLXSN-CGRP) in serum-free RPMI-1640 medium for 11 hours. At the end of this time, the samples were washed twice with phosphate-buffered saline. Adherent hCMEC/D3 cells were trypsinized to detach from the Petri dish, and subsequently resuspended in ice-cold phosphate-buffered saline. The fluorescent cells bearing PI-labeled complexes were then measured from 20,000 cells using an Epics XL flow cytometer (Beckman Coulter) in the FL3 channel.

Data analysis was performed using Epics XL flow cytometer software, and analytical gates were chosen as 1% of control cells falling within the positive region.

In vitro transduction of endothelial cells

For the transgene expression measurements, 2×10^5 hCMEC/D3 cells were seeded per well in triplicate for each sample in six-well plates. After 24 hours of culture, the cells were washed twice with phosphate-buffered saline, and 1 mL of serum-free RPMI-1640 medium containing an appropriate volume of transduction solution from the different experimental groups (naked pLXSN-CGRP, GS NP-pLXSN-CGRP, Tat-GS NP-pLXSN-CGRP) was added to the corresponding set of wells.

After transfection for up to 11 hours, the wells were replenished with complete RPMI-1640 medium containing 10% fetal bovine serum and grown at 37°C in a 5% CO_2 incubator. For experiments where CGRP transgenes were used, the conditioned medium was collected at regular intervals for 10 days and stored at −20°C for CGRP enzyme-linked immunosorbent assay (Shanghai Westang Bio-Tech Co, Ltd, Shanghai, People's Republic of China) analysis following the manufacturer's protocol. The conditioned medium released from transduced hCMEC/D3 cells after 48 hours was used for the biological assays of the CGRP released.

In vivo experiments in subarachnoid hemorrhage rat model

Fifty male Sprague-Dawley rats weighing 280–330 g were randomly assigned to one of four groups, ie, normal controls (without subarachnoid hemorrhage, n = 5), subarachnoid hemorrhage + vehicle (phosphate-buffered saline only as a nanoparticle-free control, n = 15), subarachnoid hemorrhage + Tat-GS NP-pLXSN-CGRP (n = 15), and subarachnoid hemorrhage + Tat-GS NP-pLXSN (n = 15). The double-hemorrhage rat model was induced according to a minimally invasive protocol.[14] All procedures were in compliance with the protocols evaluated and approved by the Chinese National Science and Technology Committee guidelines.

The rats were anesthetized by intraperitoneal administration of midazolam 1 mg/kg and ketamine 100 mg/kg. Next, 0.2 mL of arterial blood was taken from the tail artery. Following intra-arterial blood collection, the animals were fixed in the prone position with the head flexed 90 degrees to horizontal and the cisterna magna was punctured with a 27-gauge needle. After withdrawal of 0.1 mL of cerebrospinal fluid, 0.25 mL of autologous blood was infused into the cisterna magna by microinjection pump over a 60-second period on days 0 and 2. The animals were then kept in a head-down position until awaking from anesthesia to ensure wide subarachnoid distribution of the arterial blood. On day 3, 0.1 mL of Tat-GS NP-pLXSN-CGRP (1 mg/mL), Tat-GS NP-pLXSN (1 mg/mL), or phosphate-buffered saline was administered into the cisterna magna of the corresponding group, after which the rats were placed in the head-down position for 30 minutes. On day 7, the cerebrospinal fluid was collected from the cisterna magna of each group and analyzed by enzyme-linked immunosorbent assay for rat CGRP according to the manufacturer's instructions (Shanghai Westang Bio-Tech Co, Ltd). All the animals in the first group were sacrificed without being subjected to subarachnoid hemorrhage as a normal control group for histological study.

Neurological evaluation after subarachnoid hemorrhage

Neurological scoring was performed daily on each animal after subarachnoid hemorrhage. The scoring system (score range 0–48, 0 = best score and 48 = worst score) was based on assessment of four different functions (general status, simple motor, complex motor, and sensory), as described elsewhere.[15] These four assessments were summed into one score. An investigator blinded to group assignment did the evaluation.

Morphometric studies

After collection of cerebrospinal fluid on day 7, the rats were perfused via a cardiac catheter with 100 mL of phosphate-buffered saline 0.1 mol/L (pH 7.4) followed by 200 mL of paraformaldehyde 4% at a perfusion pressure of 120 cm H_2O. The entire brain was removed immediately from each rat and post-fixed in 4% paraformaldehyde for 24 hours. A sample of the basilar artery was removed from the brain along with the surrounding tissue and stored in 4% paraformaldehyde at 4°C. Pieces of basilar artery were dehydrated in graded ethanol, embedded in paraffin, cut into sections 4 µm thick using a manual rotary microtome (Leica RM2125, Leica Microsystems, Wetzlar, Germany) and stained with hematoxylin and eosin for light microscopy study. Morphometric determinations of luminal perimeter and vessel wall thickness were made using an Image-Pro Plus analysis system attached to a light microscope (SZ51, Olympus Corporation, Tokyo, Japan). The luminal perimeter was measured by tracing the entire luminal surface of the intima. Vessel wall thicknesses were determined by making four measurements of each artery

that extended from the luminal surface of the intima to the outer limits of the media, and did not include the adventitia.[16] These four measurements were averaged into one score.

Statistical analysis

All data are presented as the mean ± standard deviation. The Statistical Package for the Social Sciences version 13.0 (SPSS Inc, Chicago, IL, USA) was used for statistical analysis of the data. The measurements were statistically evaluated using one-way analysis of variance followed by the Bonferroni-Dunn post hoc test. A value of $P < 0.05$ was considered to be statistically significant.

Results

Characterization of nanoparticles

The strategy used for synthesis of the Tat-GS nanoparticles developed here is shown in Scheme 1. GS nanoparticles were prepared using a conventional sol-gel procedure with a 3-glycidoxypropyl-trimethoxysilane and gelatin solution. The N-succinimidyl-3-(2-pyridyldithio) propionate reagents are a unique group of amine-reactive and sulfhydryl-reactive heterobifunctional crosslinkers. Here they were used to form amine-to-sulfhydryl crosslinks among primary amine-containing GS nanoparticles and a sulfhydryl-containing

Tat peptide. Finally, the Tat peptide (KYGRRRQRRKKRGC) was attached to the GS nanoparticles via a disulfide bond.

The fluorescence emission spectrum shows an obvious fluorescence absorption peak for the FITC-Tat-GS nanoparticle suspension at 520 nm, but a weak fluorescence absorption peak for the first supernatant and nearly no fluorescence absorption peak for the second supernatant at 520 nm (Figure 1). The GS nanoparticles were not fluorescent, and the fluorescence absorption peak at 520 nm represents the FITC-labeled Tat peptide, indicating that the Tat peptide was successfully integrated onto the GS nanoparticles. Transmission electron microscopy shows that both the GS and Tat-GS nanoparticles were irregular, spherical, and well dispersed (Figure 2). The nanoparticles were characterized by measuring the particle size and zeta potential (Figure 3). The sizes of the GS nanoparticles and Tat-GS nanoparticles were 169 ± 7 nm and 172 ± 5 nm, respectively. Zeta potential measurement showed the charge values of the GS nanoparticles and Tat-GS nanoparticles to be 25.79 ± 2.46 mV and 36.28 ± 2.74 mV, respectively.
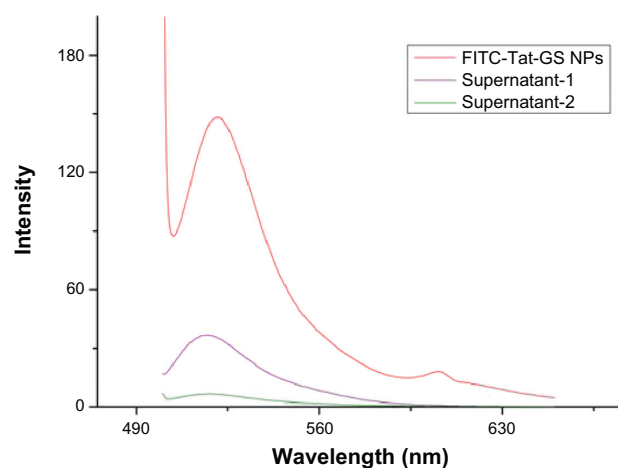
pLXSN-CGRP encapsulation

The entrapment efficiency of the nanoparticles containing pLXSN-CGRP was evaluated using agarose gel electrophoresis.
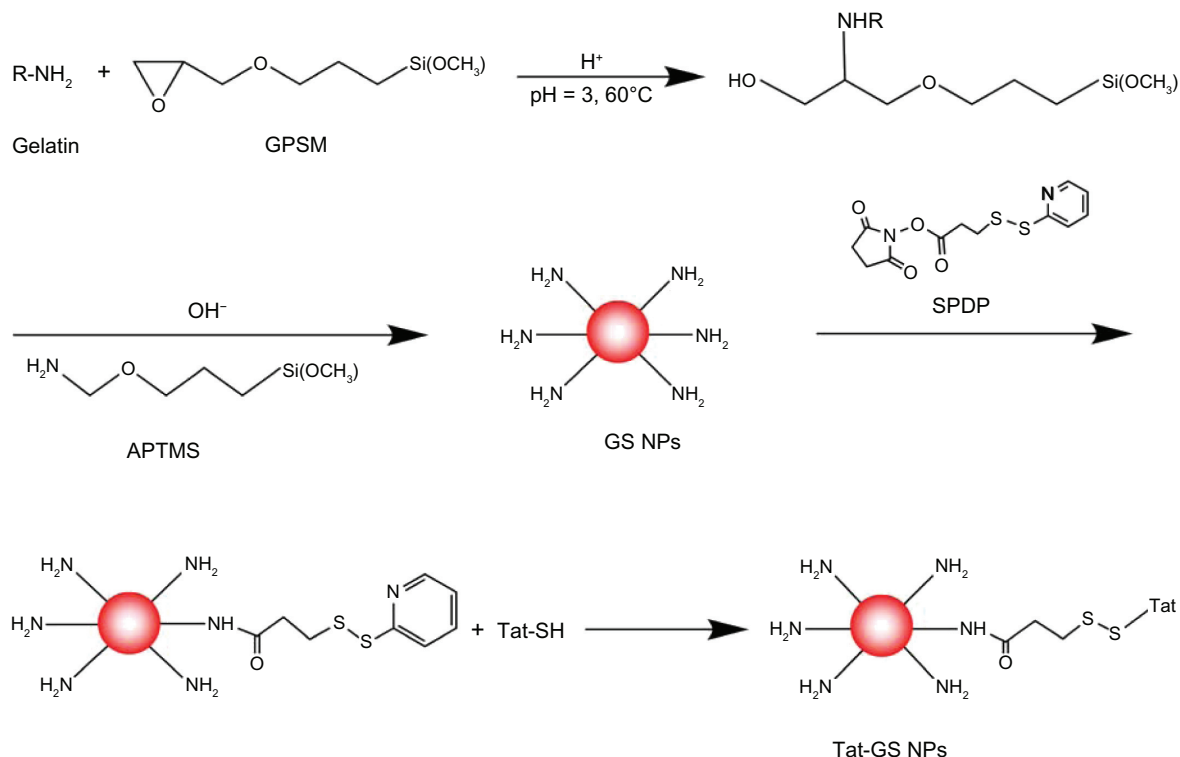
Scheme 1 Synthesis of gelatin-siloxane nanoparticles coated with Tat peptide.
Abbreviations: APTMS, 3-aminopropyltrimethoxysilane; Tat-GS, Tat peptide-decorated gelatin-siloxane; NPs, nanoparticles.

Figure 1 Fluorescence emission spectrum of FITC-Tat-GS nanoparticles excited at a wavelength of 490 nm.
Abbreviations: FITC, fluorescein isothiocyanate; NPs, nanoparticles; Tat-GS, Tat peptide-decorated gelatin-siloxane.
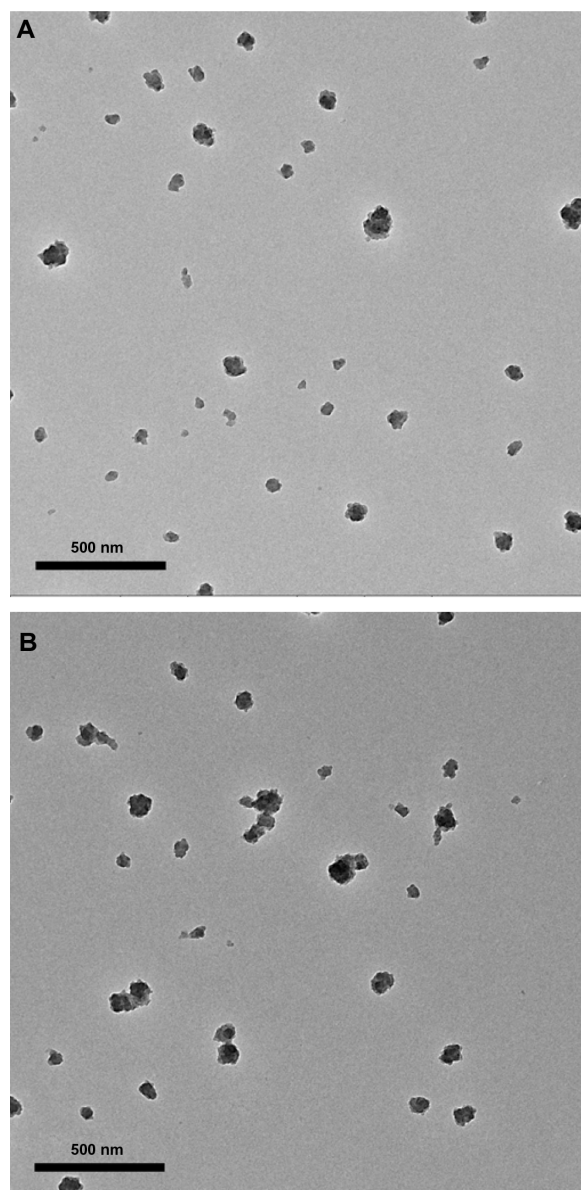

Figure 2 Transmission electron microscopic images of (**A**) gelatin-siloxane nanoparticles and (**B**) Tat-gelatin-siloxane nanoparticles.

As shown in Figure 4, naked plasmid (pLXSN-CGRP) moved to its normal position, but plasmids complexed with GS nanoparticles and Tat-GS nanoparticles were completely retarded in the walls without any band in the corresponding position. pLXSN-CGRP was encapsulated into nanoparticles with a high entrapment efficiency of approximately 100%. There was no difference in entrapment efficiency between the GS and Tat-GS nanoparticles.

Cellular compatibility

Cytotoxicity associated with the GS and Tat-GS nanoparticles was measured using the MTT assay. As shown in Figure 5, the viability of hCMEC/D3 cells treated with GS nanoparticles for 24 hours was 91.57%, 88.77%, and 85.87% at nanoparticle concentrations of 100 μg/mL, 300 μg/mL, and 500 μg/mL, respectively. Viability of cells treated with Tat-GS nanoparticles was 81.33%, 79.93%, and 74.88%, respectively. The viability of hCMEC/D3 cells treated with Tat-GS nanoparticles, under the same conditions, was less than that of the cells treated with GS nanoparticles. Nevertheless, both the as-synthesized nanoparticles had quite low cytotoxicity at a concentration of 100 μg/mL.

Cellular uptake of nanoparticles

Flow cytometry analysis was used to evaluate whether plasmid pLXSN-CGRP loaded into the nanoparticles could be internalized by hCMEC/D3 cells and for quantitative assessment of plasmid-containing hCMEC/D3 cells in vitro. As shown in Figure 6A, the peak values of fluorescence curves obtained for hCMEC/D3 cells transfected with PI-labeled GS NP-pLXSN-CGRP and PI-labeled Tat-GS NP-pLXSN-CGRP were

clearly shifted to the right compared with the naked PI-labeled pLXSN-CGRP group. Figure 6B shows significant uptake of PI-labeled GS NP-pLXSN-CGRP (62.97% ± 4.54%) and PI-labeled Tat-GS NP-pLXSN-CGRP (65.60% ± 5.14%) by hCMEC/D3 cells compared with the naked PI-labeled pLXSN-CGRP group (1.82% ± 0.13%). There was no statistically significant difference between the values for the GS group and the Tat-GS group ($P > 0.05$), and neither value was significantly higher than that in the control group ($P < 0.01$).

Induction of CGRP expression in vitro

To confirm the ability of the pLXSN-CGRP nanoparticle complex to express the rat CGRP transgene, and to perform
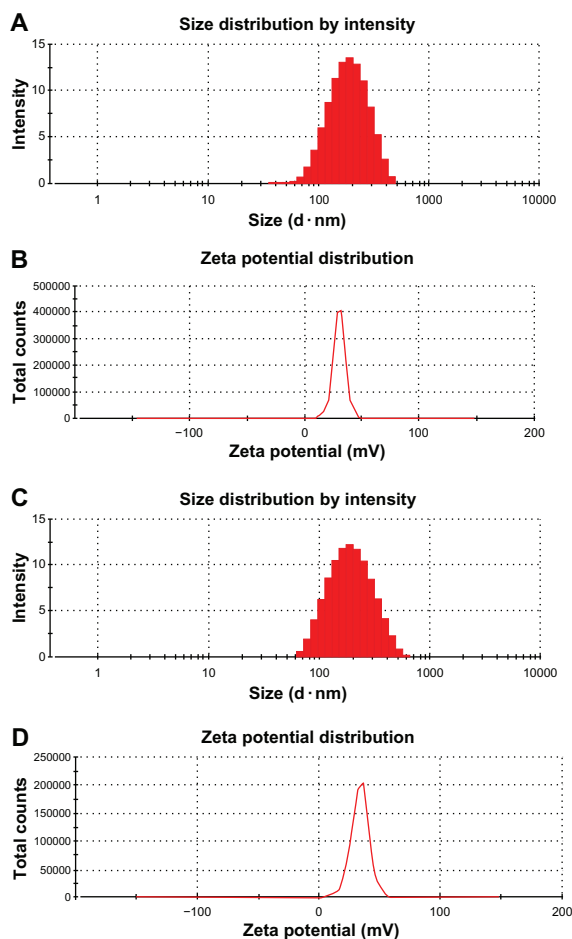
Figure 3 Physical characterization of nanoparticles. Size distribution of gelatin-siloxane nanoparticles (**A**) and Tat peptide-decorated gelatin-siloxane nanoparticles (**C**) by intensity (%). Zeta potential distribution of gelatin-siloxane nanoparticles (**B**) and Tat-gelatin-siloxane nanoparticles (**D**) by total counts.
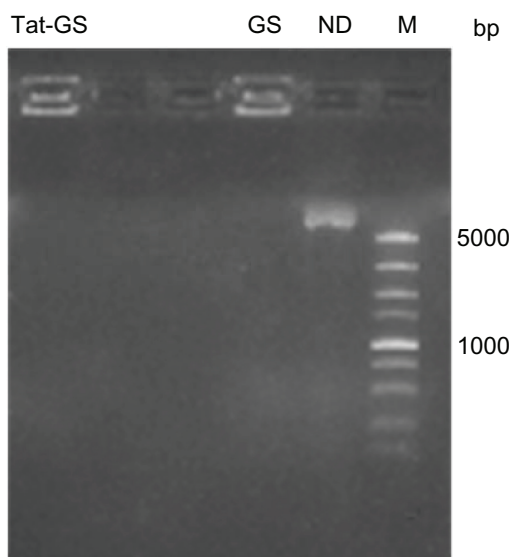
Figure 4 Gel electrophoresis assay of NP-pLXSN-CGRP complexes.
Abbreviations: bp, base pairs; M, DL 5000 DNA marker; ND, naked DNA (pLXSN-CGRP); GS, gelatin-siloxane nanoparticles; Tat-GS, Tat peptide-decorated gelatin-siloxane nanoparticles.
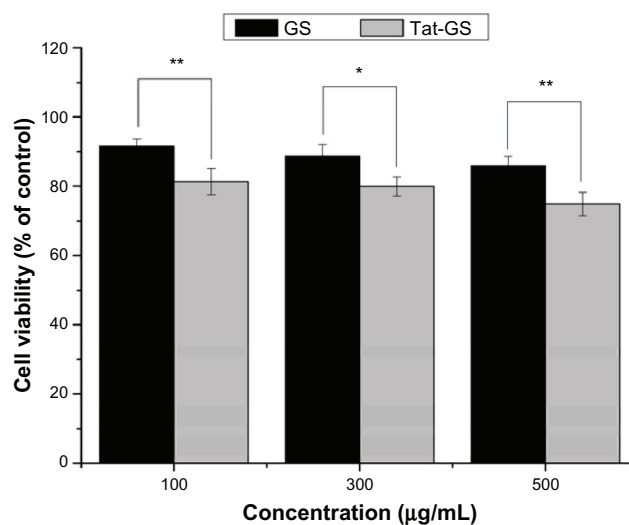
Figure 5 Normalized dose-response for cell viability of GS and Tat-GS nanoparticles by MTT assay.
**Notes:** $**P < 0.001$; $*P < 0.01$ indicate a statistically significant difference. Values are shown as the mean $\pm$ standard deviation (n = 5).
Abbreviations: GS, gelatin-siloxane nanoparticles; Tat-GS, Tat peptide-decorated gelatin-siloxane nanoparticles.

the quantitative assessment of the protein by enzyme-linked immunosorbent assay, hCMEC/D3 cells were transduced with naked pLXSN-CGRP, GS NP-pLXSN-CGRP, and Tat-GS NP-pLXSN-CGRP. The data shown in Figure 7A demonstrate that the Tat-GS NP-pLXSN-CGRP group had the highest CGRP expression (40.25 ± 5.52 ng/10^5 cells) 72 hours following transduction compared with the naked pLXSN-CGRP group (5.82 ± 1.97 ng/10^5 cells) and GS NP-pLXSN-CGRP group (23.57 ± 3.93 ng/10^5 cells). There was a significant difference between the three groups. As shown in Figure 7B, the CGRP release profile for cells transduced with Tat-GS NP-pLXSN-CGRP showed rapid expression of the CGRP transgene, which peaked on day 4 (48.49 ± 4.23 ng/10^5 cells), then gradually decreased with time, as observed in the 10-day analysis.

Intracisternal delivery of CGRP transgene in vivo

To confirm and quantify rat CGRP expression in vivo, cerebrospinal fluid obtained on day 7 from each group was measured by CGRP enzyme-linked immunosorbent assay. As shown in Figure 8, the untreated rats with subarachnoid hemorrhage showed decreased CGRP expression in cerebrospinal fluid (23.82 ± 1.28 ng/L) compared with normal rats (27.68 ± 0.67 ng/L). However, the Tat-GS NP-pLXSN-CGRP group expressed significantly more protein in cerebrospinal fluid (35.40 ± 1.36 ng/L) than the Tat-GS NP-pLXSN group (23.10 ± 1.63 ng/L) and the subarachnoid hemorrhage group.
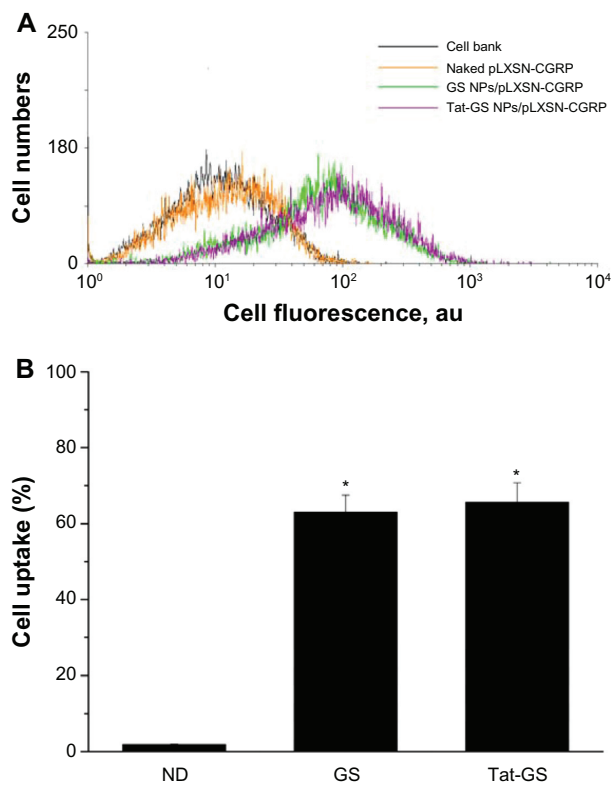
Figure 6 Uptake of propidium iodide-labeled pLXSN-CGRP by hCMEC/D3 cells incubated with naked propidium iodide-labeled pLXSN-CGRP, propidium iodide-labeled GS NP-pLXSN-CGRP, and propidium iodide-labeled Tat-GS NP-pLXSN-CGRP for 11 hours, as determined by flow cytometry.
Notes: Values are expressed as the mean ± standard deviation (n = 4). *$P < 0.01$ versus naked propidium iodide-labeled pLXSN-CGRP.
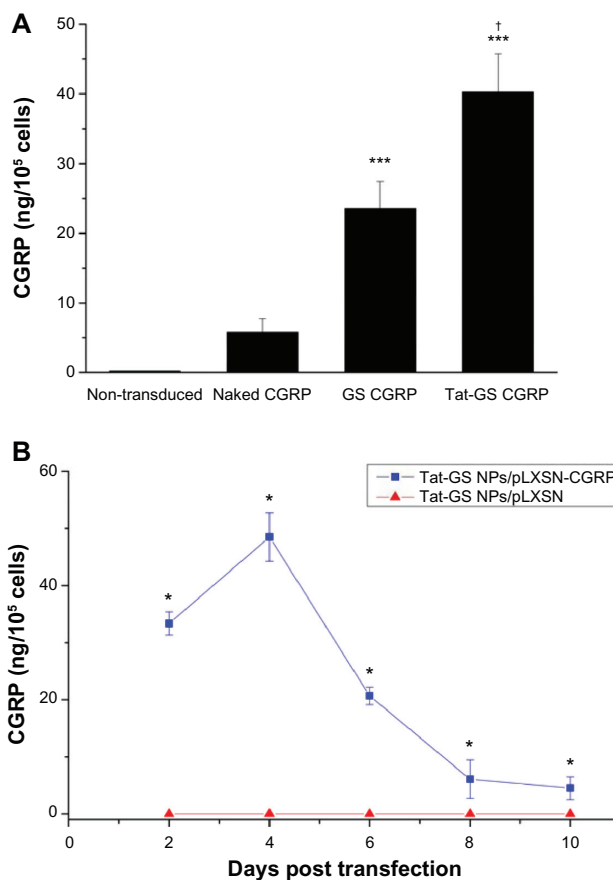**Abbreviations:** ND, naked DNA (pLXSN-CGRP); GS, gelatin-siloxane nanoparticles; Tat-GS, Tat peptide-decorated gelatin-siloxane nanoparticles.

Neurological evaluation following subarachnoid hemorrhage

This experiment investigated whether intracisternal administration of Tat-GS NP-mediated gene therapy resulted in improved neurological outcome. A comprehensive neurological scoring system was administered three times daily in each rat. As shown in Figure 9, the mean neurological score on day 7 for the Tat-GS NP-pLXSN-CGRP-treated group (10.67 ± 1.16) was significantly lower than that for the Tat-GS NP-pLXSN-treated group (22.33 ± 2.08; $P < 0.001$) and the subarachnoid hemorrhage group (20.67 ± 1.16; $P < 0.001$). Further, no statistically significant differences were found between the Tat-GS NP-pLXSN-treated group and the subarachnoid hemorrhage group ($P > 0.05$).

Morphometric results

Figure 10A–D shows light microscopic pictures of the basilar arteries from the control group and the subarachnoid hemorrhage group. Different degrees of vasospasm were observed in both the treated and untreated subarachnoid


Figure 7 Effect of NP-pLXSN-CGRP gene delivery system on CGRP protein expression in hCMEC/D3 cells. (**A**) CGRP concentrations as measured by enzyme-linked immunosorbent assay 72 hours following transduction. (**B**) Time course release profile for CGRP from Tat-GS NP-pLXSN-CGRP-transduced hCMEC/D3 cells over 10 days.
Notes: ***$P < 0.001$ versus naked pLXSN-CGRP; *$P < 0.001$ versus Tat-GS NP-pLXSN; †$P < 0.001$ versus GS CGRP. Values are shown as the mean ± standard deviation (n = 6).
Abbreviations: GS, gelatin-siloxane nanoparticles; NPs, nanoparticles; Tat-GS, Tat peptide-decorated gelatin-siloxane nanoparticles.

hemorrhage rats, including luminal narrowing, increased wall thickness, and corrugation of the internal elastic lamina in the basilar arteries. Meanwhile, all the subarachnoid hemorrhage rats, including those treated with Tat-GS NP-pLXSN or Tat-GS NP-pLXSN-CGRP, developed morphometric vasospasm as shown by the quantitative bar graphs in Figure 10E and F. The mean perimeters of the basilar arteries, as a percentage of that measured in the normal control group, were 56% ± 4%, 51% ± 6%, and 74% ± 7%, for the subarachnoid hemorrhage, Tat-GS NP-pLXSN, and Tat-GS NP-pLXSN-CGRP groups, respectively. Compared with the subarachnoid hemorrhage group, the Tat-GS NP-pLXSN-CGRP group showed a significant increase in the luminal perimeter of the basilar artery ($P < 0.001$), but the Tat-GS NP-pLXSN group did not ($P > 0.05$). Corresponding measurements of wall thickness were 248% ± 13%,
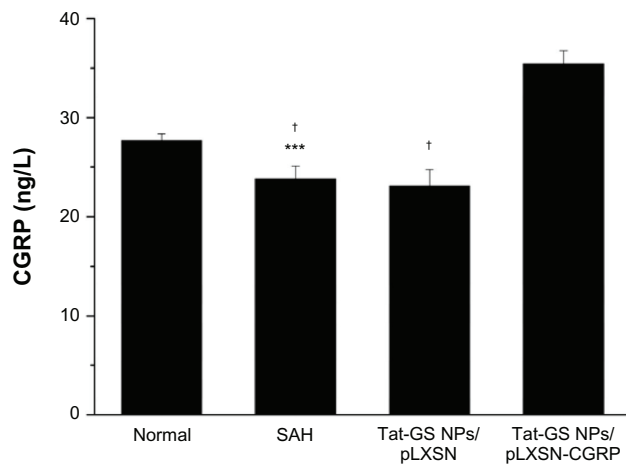
Figure 8 Quantitative assessment of rat CGRP in cerebrospinal fluid on day 7 by rat CGRP enzyme-linked immunosorbent assay.
**Notes:** ***$P < 0.001$ versus normal; †$P < 0.001$ versus Tat-GS NP-pLXSN-CGRP. Mean values $\pm$ standard deviation are shown (n = 15).
Abbreviations: NPs, nanoparticles; Tat-GS, Tat peptide-decorated gelatin-siloxane nanoparticles; SAH, subarachnoid hemorrhage.

269% ± 20%, and 193% ± 14%, respectively. However, while the 193% ± 14% wall thickness in the Tat-GS NP-pLXSN-CGRP group represented a significant change from the subarachnoid hemorrhage group, the 269% ± 20% wall thickness in the Tat-GS NP-pLXSN group did not.

Discussion

Steady progress in experimental gene therapy for cerebral vasospasm has been made over the past decade. However, inflammatory and immune responses to virus vectors are still major obstacles to effective gene therapy for vasospasm after
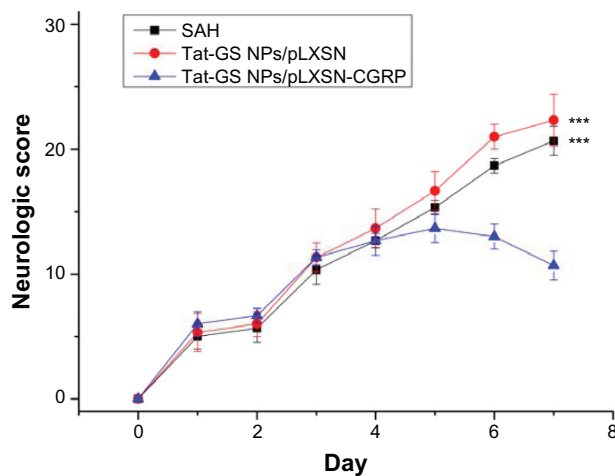
Figure 9 Line graph showing the effect of CGRP transgene on neurological scores.
Notes: The Tat-GS NP-pLXSN-CGRP-treated group had significantly improved neurological scores compared with the SAH and Tat-GS NP-pLXSN-treated groups. ***$P < 0.001$ versus Tat-GS NP-pLXSN-CGRP-treated groups.
Abbreviations: NPs, nanoparticles; SAH, subarachnoid hemorrhage; Tat-GS, Tat peptide-decorated gelatin-siloxane nanoparticles.
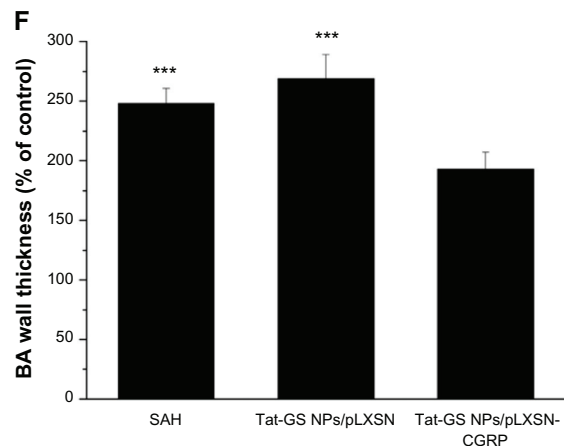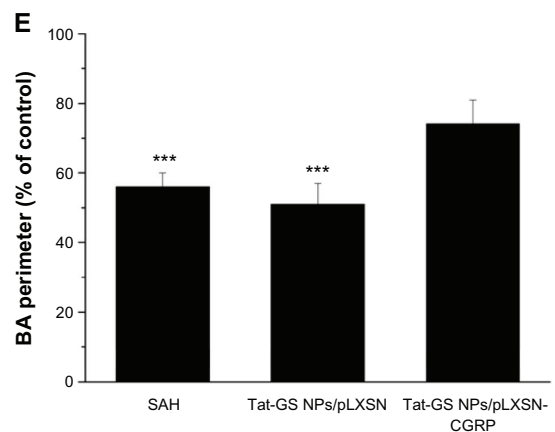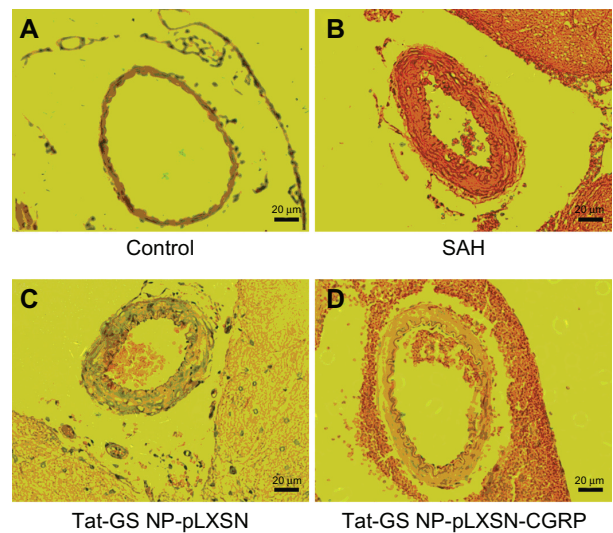
Figure 10 Morphometric changes in the basilar arteries after subarachnoid hemorrhage. (**A–D**) Representative light photomicrographs of the basilar arteries. Typical histological features of cerebral vasospasm were shown in the subarachnoid hemorrhage and Tat-GS NP-pLXSN groups, demonstrated by corrugation of the internal elastic lamina, luminal narrowing, and increased wall thickness. (**E**) Perimeter of lumen of basilar arteries. (**F**) Wall thickness of vessels.
Notes: Hematoxylin and eosin staining 200×. Scale bars 20 μm. The significant increase in vessel perimeters with a corresponding decrease in wall thickness is shown in the Tat-GS NP-pLXSN-CGRP group as compared with the SAH group. Control values taken from the normal control group are considered 100%. ***$P < 0.001$ versus Tat-GS NP-pLXSN-CGRP group.
Abbreviations: Tat-GS, Tat peptide-decorated gelatin-siloxane nanoparticles; SAH, subarachnoid hemorrhage.

subarachnoid hemorrhage. Nonviral vectors, especially the nanoparticle vector with its low immunogenicity and good biocompatibility, have been reported to have beneficial effects in gene delivery in vitro and in vivo.[10,17] In this paper, we report application of a vasodilator gene carried by nanoparticles for the potential treatment of cerebral vasospasm. For this, we developed a Tat peptide-decorated GS nanoparticle carrying CGRP and investigated its potential for transducing endothelial cells and eventually inducing efficient therapeutic vasodilation and neuroprotection. Figures 1–3 confirm successful formation of Tat-GS nanoparticles using transmission electron microscopy, particle size, zeta potential, and quantitative analysis with spectrofluorimetry.

Our data reveal that the efficiency of gene transfer can be significantly enhanced by Tat-GS nanoparticles (Figure 7A), although there were no significant differences in pLXSN-CGRP entrapment efficiency and cellular uptake between Tat-GS nanoparticles and GS nanoparticles (Figures 4 and 6). It is likely that the duration of cell incubation with the nanocomplexes is long enough for both NP-pLXSN-CGRP complexes to adhere to the cell surface and then internalize into the cell. Therefore, Tat-GS and GS nanoparticles have parallel efficiency in terms of cellular uptake. The Tat peptide is characterized by a linear sequence of 13 amino acids which carries a transmembrane signal and a nuclear localization signal.[18,19] Membrane penetration is driven primarily by ionic interaction between the cationic charges of the Tat peptide and the anionic charges of the phospholipid heads in the biomembrane. Therefore, the Tat peptide is used extensively for mediating intracellular delivery of many different types of cargos,[20] including GS nanoparticles.[13]

The early literature indicated that internalized Tat-GS nanoparticles might first be trapped in endosomes, and then escape from endocytic vesicles via membrane fusion or a proton sponge effect.[11,21] Because of the effect of the nuclear localization signal in the Tat peptide, pLXSN-CGRP loaded into Tat-GS nanoparticles can be transferred into the nucleus, so that the pLXSN-CGRP can be protected until its entry into the nucleus and then be released from the Tat-GS nanoparticles for efficient gene transfection. In vitro analysis showed that cells transduced by Tat-GS nanoparticles can express their transgene for at least ten days and reach a peak on day 4 (Figure 7B). In the rat model of subarachnoid hemorrhage, vasospasm usually peaks approximately 5 days after the second injection of blood.[14,16,22] Therefore, when injecting Tat-GS NP-pLXSN-CGRP into the cisterna magna in rats with subarachnoid hemorrhage one day following the

second injection of blood, the time course of overexpression of CGRP may coincide with the onset of vasospasm. After performing the therapeutic experiments in vivo, we compared and confirmed superior expression of the Tat-GS nanoparticle delivery systems by measuring CGRP expression levels in cerebrospinal fluid (Figure 8). The data show that a single injection of Tat-GS NP-pLXSN-CGRP enabled continuous production and accumulation of CGRP in cerebrospinal fluid, with a vasodilatory effect.

Over the last decade, although many genes have been used for experimental gene therapy in vasospasm, and some have been considered to be useful, researchers finally concluded that CGRP gene transfer might be one of the most promising.[23–27] Previous researchers have studied the effect of CGRP gene therapy in the treatment of cerebrovascular disease. A study by Toyoda et al reported that the therapeutic effect of CGRP overexpression in a single blood injection rabbit model was prevention of cerebral vasospasm.[4] Further, a study using a double-hemorrhage dog model demonstrated that application of adenovirus-mediated gene transfer of CGRP attenuated cerebral vasospasm after subarachnoid hemorrhage.[3] Our study using Tat-GS nanoparticles also had positive results, clearly improving neurological scores (Figure 9) and demonstrating a significant increase in vessel perimeters and a corresponding decrease in wall thickness of the basilar artery (Figure 10). This amelioration of cerebral vasospasm and the associated behavioral outcome may result from the fact that CGRP protects tissue from injury in addition to having a vasodilatory effect on cerebral vessels. There is also evidence for a protective role of endogenous CGRP from a pig model of myocardial infarction,[28] possibly via protection of microvascular endothelial cells,[29] and that CGRP is a potent microvascular vasodilator, regulating microvascular blood flow and increasing tissue perfusion to protect tissue from injury. This is consistent with the results of our study, which demonstrated a consistent reduction in histologically determined vasospasm and an improved functional outcome.

In our preclinical study of this novel Tat-GS nanoparticle vector, we characterized the nanocomplex, optimized the in vitro gene delivery protocol used in a previous study, and evaluated its therapeutic potential using a double-hemorrhage rat model. Further work needs to be done to develop strategies for targeting appropriate tissue and regulating gene expression, which will augment the efficacy of gene transfer. This may be achieved by using a specific promoter sequence or functionalizing the surface of the nanoparticle with targeting ligands to prevent expression

at nonspecific sites.[30–32] In addition to exploring the pharmacodynamics of nanocomplexes, the pharmacokinetics of the vector and any potential adverse reactions caused by overexpression of the CGRP gene must also be clarified.[33]

However, some limitations remain. Long-term neurocognitive deficits are often seen in patients with vasospasm in clinical practice, so integrating the long-term tasks of learning and memory into our neurological scoring system might further improve the clinical relevance of this study.[34] Further, given that there are documented anatomical differences between the cerebral arteries of the rat and those of humans,[35–37] our experimental model of subarachnoid hemorrhage in rats does not fully replicate vasospasm after subarachnoid hemorrhage in humans. Further studies using larger or even primate models of vasospasm are needed to address this limitation.

Conclusion

This study demonstrates the unique potential of Tat-GS nanoparticles in gene delivery and suggests a potential role for these nanoparticles in treating cerebral vasospasm. Our data show that loading of the CGRP gene into Tat-GS nanoparticles can attenuate vasospasm after subarachnoid hemorrhage and improve the neurological outcome. In addition to its vasodilatory effect in the cerebral vessels, CGRP may also act as a neuroprotective agent. Use of the CGRP gene and Tat-GS nanoparticles is a safe and effective gene delivery system for the treatment of cerebral vasospasm.

Acknowledgments

Disclosure

The authors report no conflicts of interest in this work.

References

1. Seiler RW, Grolimund P, Zurbruegg HR. Evaluation of the calcium-antagonist nimodipine for the prevention of vasospasm after aneurysmal subarachnoid haemorrhage. A prospective transcranial Doppler ultrasound study. *Acta Neurochir (Wien)*. 1987;85(1–2):7–16.
2. Brain SD, Grant AD. Vascular actions of calcitonin gene-related peptide and adrenomedullin. *Physiol Rev*. 2004;84(3):903–934.
3. Satoh M, Perkins E, Kimura H, et al. Post treatment with adenovirus-mediated gene transfer of calcitonin gene-related peptide to reverse cerebral vasospasm in dogs. *J Neurosurg*. 2002;97(1): 136–142.
4. Toyoda K, Faraci FM, Watanabe Y, et al. Gene transfer of CGRP prevents vasoconstriction after subarachnoid hemorrhage. *Circ Res*. 2000;87(9):818–824.
5. Mesis RG, Wang H, Lombard FW, et al. Dissociation between vasospasm and functional improvement in a murine model of subarachnoid hemorrhage. *Neurosurg Focus*. 2006;21(3):E4.
6. Driesse MJ, Esandi MC, Kros JM, et al. Intra-CSF administered recombinant adenovirus causes an immune response-mediated toxicity. *Gene Ther*. 2000;7(16):1401–1409.
7. Driesse MJ, Kros JM, Avezaat CJJ, et al. Distribution of recombinant adenovirus in the cerebrospinal fluid of nonhuman primates. *Hum Gene Ther*. 1999;10(14):2347–2354.
8. Dang JM, Leong KW. Natural polymers for gene delivery and tissue engineering. *Adv Drug Deliv Rev*. 2006;58(4):487–499.
9. Luo D, Han E, Belcheva N, Saltzman WM. A self-assembled, modular DNA delivery system mediated by silica nanoparticles. *J Control Release*. 2004;95(2):333–341.
10. Bharali DJ, Klejbor I, Stachowiak EK, et al. Organically modified silica nanoparticles: a nonviral vector for in vivo gene delivery and expression in the brain. *Proc Natl Acad Sci U S A*. 2005;102(32):11539–11544.
11. Wang ZY, Zhao Y, Ren L, et al. Novel gelatin-siloxane nanoparticles decorated by Tat peptide as vectors for gene therapy. *Nanotechnology*. 2008;19(44):445103.
12. Tian XH, Wei F, Wang TX, et al. In vitro and in vivo studies on gelatin-siloxane nanoparticles conjugated with SynB peptide to increase drug delivery to the brain. *Int J Nanomedicine*. 2012;7:1031–1041.
13. Tian XH, Wei F, Wang TX, et al. Blood-brain barrier transport of Tat peptide and polyethylene glycol decorated gelatin-siloxane nanoparticles. *Mater Lett*. 2012;68:94–96.
14. Dusick JR, Evans BC, Laiwalla A, Krahl S, Gonzalez NR. A minimally-invasive rat model of subarachnoid hemorrhage and delayed ischemic injury. *Surg Neurol Int*. 2011;2:99.
15. Yokoo N, Sheng H, Mixco J, Homi HM, Pearlstein RD, Warner DS. Intraischemic nitrous oxide alters neither neurologic nor histologic outcome: a comparison with dizocilpine. *Anesth Analg*. 2004;99(3):896–903.
16. Meguro T, Clower BR, Carpenter R, Parent AD, Zhang JH. Improved rat model for cerebral vasospasm studies. *Neurol Res*. 2001;23(7): 761–766.
17. Surendiran A, Sandhiya S, Pradhan SC, Adithan C. Novel applications of nanotechnology in medicine. *Indian J Med Res*. 2009;130(6): 689–701.
18. Brooks H, Lebleu B, Vives E. Tat peptide-mediated cellular delivery: back to basics. *Adv Drug Deliv Rev*. 2005;57(4):559–577.
19. Berry CC. Intracellular delivery of nanoparticles via the HIV-1 tat peptide. *Nanomedicine*. 2008;3(3):357–365.
20. Song HP, Yang JY, Lo SL, et al. Gene transfer using self-assembled ternary complexes of cationic magnetic nanoparticles, plasmid DNA and cell-penetrating Tat peptide. *Biomaterials*. 2010;31(4):769–778.
21. Xu ZP, Zeng QH, Lu GQ, Yu AB. Inorganic nanoparticles as carriers for efficient cellular delivery. *Chem Eng Sci*. 2006;61(3):1027–1040.
22. Suzuki H, Kanamaru K, Tsunoda H, et al. Heme oxygenase-1 gene induction as an intrinsic regulation against delayed cerebral vasospasm in rats. *J Clin Invest*. 1999;104(1):59–66.
23. Stoodley M, Weihl CC, Zhang Z, et al. Effect of adenovirus-mediated nitric oxide synthase gene transfer on vasospasm after experimental subarachnoid hemorrhage. *Neurosurgery*. 2000;46(5):1193–1203.
24. Ohkuma H, Parney I, Megyesi J, Ghahary A, Findlay JM. Antisense preproendothelin-oligoDNA therapy for vasospasm in a canine model of subarachnoid hemorrhage. *J Neurosurg*. 1999;90(6):1105–1114.
25. Ono S, Date I, Onoda K, et al. Decoy administration of NF-κB into the subarachnoid space for cerebral angiopathy. *Hum Gene Ther*. 1998;9(7): 1003–1011.
26. Ono S, Komuro T, Macdonald RL. Heme oxygenase-1 gene therapy for prevention of vasospasm in rats. *J Neurosurg*. 2002;96(6): 1094–1102.
27. Yamaguchi M, Zhou C, Heistad DD, Watanabe Y, Zhang JH. Gene transfer of extracellular superoxide dismutase failed to prevent cerebral vasospasm after experimental subarachnoid hemorrhage. *Stroke*. 2004;35(11):2512–2517.

28. Kallner G, Franco-Cereceda A. Aggravation of myocardial infarction in the porcine heart by capsaicin-induced depletion of calcitonin gene-related peptide (CGRP). *J Cardiovasc Pharmacol*. 1998;32(3):500–504.

29. Li YJ, Song QJ, Xiao J. Calcitonin gene-related peptide: an endogenous mediator of preconditioning. *Acta Pharmacol Sin*. 2000;21(10):865–869.

30. Su H, Joho S, Huang Y, et al. Adeno-associated viral vector delivers cardiac-specific and hypoxia-inducible VEGF expression in ischemic mouse hearts. *Proc Natl Acad Sci U S A*. 2004;101(46):16280–16285.

31. Medley CD, Bamrungsap S, Tan W, Smith JE. Aptamer-conjugated nanoparticles for cancer cell detection. *Anal Chem*. 2011;83(3):727–734.

32. Dhar S, Gu FX, Langer R, Farokhzad OC, Lippard SJ. Targeted delivery of cisplatin to prostate cancer cells by aptamer functionalized Pt(IV) prodrug-PLGA-PEG nanoparticles. *Proc Natl Acad Sci U S A*. 2008;105(45):17356–17361.

33. Pislaru S, Janssens SP, Gersh BJ, Simari RD. Defining gene transfer before expecting gene therapy: putting the horse before the cart. *Circulation*. 2002;106(5):631–636.

34. Shimamura M, Sato N, Waguri S, et al. Gene transfer of hepatocyte growth factor gene improves learning and memory in the chronic stage of cerebral infarction. *Hypertension*. 2006;47(4):742–751.

35. Gules I, Saton M, Clower BR, Nanda A, Zhang JH. Comparison of three rat models of cerebral vasospasm. *Am J Physiol Heart Circ Physiol*. 2002;283(6):H2551–H2559.

36. Frederickson RG, Low FN. Blood vessels and tissue space associated with the brain of the rat. *Am J Anat*. 1969;125(2):123–145.

37. Kader A, Krauss WE, Onesti ST, Elliott JP, Solomon RA. Chronic cerebral blood flow changes following experimental subarachnoid hemorrhage in rats. *Stroke*. 1990;21(4):577–581.